creative commons
COMMONS DEED

저작자표시-비영리-변경금지 2.0 대한민국

이용자는 아래의 조건을 따르는 경우에 한하여 자유롭게

- 이 저작물을 복제, 배포, 전송, 전시, 공연 및 방송할 수 있습니다.

다음과 같은 조건을 따라야 합니다:

저작자표시. 귀하는 원저작자를 표시하여야 합니다.

비영리. 귀하는 이 저작물을 영리 목적으로 이용할 수 없습니다.

변경금지. 귀하는 이 저작물을 개작, 변형 또는 가공할 수 없습니다.

- 귀하는, 이 저작물의 재이용이나 배포의 경우, 이 저작물에 적용된 이용허락조건을 명확하게 나타내어야 합니다.
- 저작권자로부터 별도의 허가를 받으면 이러한 조건들은 적용되지 않습니다.

저작권법에 따른 이용자의 권리는 위의 내용에 의하여 영향을 받지 않습니다.

이것은 이용허락규약(Legal Code)을 이해하기 쉽게 요약한 것입니다.

Disclaimer

dCollection

이학석사 학위논문

Inhibition of WEE1 potentiates sensitivity to PARP inhibitor in biliary tract cancer

담도암에서 WEE1 억제를 통한 PARP 억제제의 항종양효과 증대

2021 년 8 월

서울대학교 대학원

협동과정 종양생물학 전공

융합전공 혁신의과학과

서 혜 림

Inhibition of WEE1 potentiates sensitivity to PARP inhibitor in biliary tract cancer

지도 교수 오 도 연

이 논문을 이학석사 학위논문으로 제출함
2021 년 4 월

서울대학교 대학원
협동과정 종양생물학 전공
융합전공 혁신의과학과
서 혜 림

서혜림의 이학석사 학위논문을 인준함
2021 년 7 월

위 원 장 _____

부위원장 _____

위 원 _____

Abstract

Inhibition of WEE1 potentiates sensitivity to PARP inhibitor in biliary tract cancer

Hyerim Seo

Interdisciplinary Program in Cancer Biology Major

Integrated Major in Innovative Medical Science

The Graduate School

Seoul National University

Purpose: Up to 20% of patients with biliary tract cancer (BTC) have alterations in DNA damage response (DDR) genes, including homologous recombination (HR) genes. Therefore, the DDR pathway could be a promising target for new drug development in BTC. PARP inhibitor disrupts single-strand break (SSB) repair and this SSB converses to double-strand break (DSB). On the other

hand, WEE1 inhibitor disrupts the G2/M checkpoint and HR repair. For this reason, we tested the olaparib to BTC and aim to investigate the anti-tumor effects using PARP and WEE1 inhibitors in BTC.

Materials and Methods: We used 10 biliary tract cancer cell lines to evaluate an anti-tumor effect of olaparib (a PARP inhibitor) and AZD1775 (a WEE1 inhibitor) in *in vitro*. We performed MTT assay, western blotting, and cell cycle analysis to examine the olaparib effect. Colony forming assay, alkaline comet assay, and annexin V/PI apoptosis assay were used to analyze the combination synergy. We performed p-HH3 staining assay to detect the mitotic cells and performed immunofluorescence assay to detect the RAD51 foci. Additionally, we established SNU869 xenograft model for *in vivo* experiments and conducted immunohistochemistry with tumor tissues.

Results: In this study, we observed a modest anti-proliferative effect of olaparib. DNA double-strand break (DSB) and apoptosis were increased by olaparib in BTC cells. We observed that the protein expressions of γ-H2AX, cleavage of caspase-7, and cleavage of caspase-3 were increased. However, we observed the G2 arrest by olaparib through cell cycle assay, and G2/M progress

markers, p-CDK1 and Cyclin B1, also increased. Furthermore, we observed the CtIP, RAD51, and NBS1 expression were increased by olaparib. It showed olaparib-induced DNA DSB was repaired through the HR pathway, and G2 arrest was induced to secure the time for repair. As AZD1775 typically regulates the G2/M checkpoint, we combined olaparib with AZD1775 to abrogate G2 arrest. We observed that AZD1775 downregulated p-CDK1, a G2/M cell cycle checkpoint protein, and induced early mitotic entry. AZD1775 also decreased CtIP and RAD51 expression and disrupted HR repair. In xenograft model, olaparib plus AZD1775 treatment reduced tumor growth more potently than did monotherapy with either drug.

Conclusion: This is the first study to suggest that olaparib combined with AZD1775 can induce synergistic anti-tumor effects against BTC. Based on findings of G2 arrest and HR repair with Olaparib monotherapy, we added AZD1775 to disrupt DNA repair at the G2 phase by inhibiting CDK1 phosphorylation. The combination therapy that blocks dual PARP and WEE1 showed the antitumor effect in vivo test and has the potential to be further clinically developed for BTC patients.

Keywords: PARP, WEE1, Biliary tract cancer, DNA damage response, Cell cycle checkpoint, Homologous recombination

Student Number: 2019-28812

Table of Contents

List of Figures

Introduction

The DNA damage response (DDR) pathway is an essential target for cancer treatment, and the effectiveness of DDR-targeted agents has been evaluated in a variety of cancers [1]. Biliary tract cancers (BTCs) are relatively rare cancers with few systemic treatment options and have poor prognosis [2]. Thus, novel treatment strategies are urgently needed to improve the outcomes of patients with advanced BTC. Up to 20% of patients with BTC exhibit alterations in DDR genes, including homologous recombination (HR) genes. The alterations in HR genes can be targeted by olaparib, a poly-(ADP)-ribose polymerase (PARP) inhibitor [3, 4]. Olaparib is an effective therapeutic strategy for patients with breast cancer, ovarian cancer, pancreatic cancer, and prostate cancer with germline BRCA mutations [5-8]. Currently, although preclinical data on BTC with PARP inhibitors are scarce, several clinical trials involving PARP inhibitors are being tested [3].

Olaparib disrupts single-strand break (SSB) repair by trapping PARP in DNA; this disruption of SSB repair at the replication fork provokes the conversion of unrepaired SSB to a more genotoxic single-ended DSB (seDSB) [9]. Repairing DNA DSBs is essential for cell survival and is achieved via two mechanisms: non-

homologous end joining (NHEJ) repair and HR repair [10]. seDSBs can be faithfully repaired via the HR pathway in HR-proficient cancer cells, while HR repair-deficient cancer cells must rely on the less accurate NHEJ, resulting in increased genomic instability, which eventually leads to apoptosis [9, 11]. This is why HR repair is well known as an olaparib resistance mechanism [12].

Furthermore, olaparib induces G2 arrest, which allows time to repair DNA damage [13]. G2 arrest with olaparib can be induced by a p53-dependent mechanism, wherein p53 induces p21, which prevents cyclin-dependent kinase 1 (CDK1) activation, thereby regulating G2 arrest [14]. CDK1 can also be inhibited in a p53-independent manner through the ATR-CHK1-CDC25 axis [15]. Although the p53-dependent pathway is well known to be involved in olaparib-induced G2 arrest, the p53-independent mechanism has not been sufficiently investigated.

The WEE1 checkpoint kinase has been shown to control both S-phase and G2/M progression by regulating CDK1/2 [16]. The CDK1 and cyclin B complex is the main factor that determines mitotic entry [17]. WEE1 blocks CDK1 activity and activates the G2/M cell cycle checkpoint to prevent unscheduled mitosis [16]. AZD1775, a WEE1 inhibitor, increases CDK1 activity by inhibiting WEE1,

overriding the G2/M cell cycle checkpoint [18]. The premature cells in the G2 phase are forced to enter mitosis, resulting in mitotic catastrophe [19]. CDK1 also regulates HR repair through WEE1 inhibition, but the mechanism is not fully understood [20].

In this study, we aimed to investigate the combination of olaparib and AZD1775 as a new DDR-targeted therapy for BTC. We added AZD1775 to olaparib to regulate CDK1, the key molecule that causes G2 arrest in BTC, and focused on the effects of AZD1775 abrogating the G2 arrest and blocking the HR pathway to enhance the efficacy of olaparib.

Materials and Methods

1. Olaparib induced DNA damage and simultaneously activated G2/M checkpoint

1) Human cell lines and reagents

Ten human biliary tract cancer cell lines were used in this study. SNU245, SNU308, SNU478, SNU869, SNU1079, and SNU1196 cells were purchased from the Korean Cell Line Bank (Seoul, Korea). HuCCT-1 and TFK-1 cells were obtained from the RIKEN BioResource Center (Ibaraki, Japan). SNU2670 and SNU2773 cell lines were established from patient-derived cancer cells, as previously described [21]. All cell lines were cultured in RPMI-1640 medium (Welgen Inc., Gyeongsan, Korea) conta ining 10% fetal bovine serum and 10 μg/mL gentamicin and were maintained at 37° C in a 5% CO_2 atmosphere. WEE1 inhibitor (AZD1775) and PARP inhibitor (olaparib) were provided by AstraZeneca (Macclesfield, Cheshire, UK).

2) Cell viability assay

Cell viability was measured using MTT assay. First, cells were plated in 96-well plates and incubated overnight at 37° C before

the addition of olaparib and AZD1775 alone or in combination. Five days later, 50 μL of 3-(4,5-dimethylthiazol-2yl)-2,5-diphenyltetrazolium bromide (MTT) solution (Sigma-Aldrich, St. Louis, MO, USA) was added to each well and incubated for 4 h at 37° C. The MTT solution and medium were removed, and 150 μL DMSO was added to each well. The absorbance was measured at 540 nm using a VersaMax Microplate Reader (Molecular Devices), and the cell viability was calculated.

3) Western blotting

Cells were collected after treatment with olaparib, AZD1775, or both for 24 h and 72 h. The cells were washed with ice-cold phosphate-buffered saline (PBS) and lysed in RIPA buffer containing protease inhibitors for 30 min on ice. Proteins were obtained by centrifugation at 13,000 rpm for 20 min, and equal amounts were used for western blotting. Primary antibodies against the following proteins were purchased from Cell Signaling Technology (Beverley, MA, USA): PARP (#9532), caspase-3 (#9662), caspase-7 (#9492), ATR (#2790), ATM (#2873), p-ATM-Ser1981 (#5883), p-CHK1-Ser345 (#2341), p-Chk2-Thr68 (#2661), p53 (#9282), p-p53-Ser15 (#9284), p21 (#2947), WEE1 (#4936), p-cdc2-Tyr15 (#9111), cyclin B1

(#4138), CtIP (#9201), NBS1 (#3002), and p-CDC25C-Ser216 (#9528). GAPDH (#sc-25778) and RAD51 (#sc-398587) were purchased from Santa Cruz Biotechnology. The p-CDK2-Tyr15(#ab-76146) antibody was purchased from Abcam (Cambridge, UK). Anti-γ-H2AX antibody (#05-636) was obtained from Millipore (Billerica, MA, USA). p-ATR-Thr1989 (#GTX-128145) was purchased from GeneTex (Alton Pkwy Irvine, USA), and secondary antibodies were purchased from Thermo Fisher Scientific (Waltham, MA).

4) Cell cycle analysis

Treated cells were trypsinized, harvested, and fixed with 70% ethanol at 20° C for more than 2 days. Ethanol was removed, and the cells were resuspended in FACS buffer and incubated with 7 μL of RNase A (Invitrogen) (20 mg/mL) for 10 min at 37° C. Samples were stained with 13 μL of propidium iodide (PI; Sigma-Aldrich) and analyzed on a FACSCalibur flow cytometer (BD Biosciences, San Jose, CA, USA).

2. Combination therapy with olaparib and AZD1775 induced more potent DNA damage and apoptosis

1) Colony-formation assay

Cells were seeded on a 6-well plate and treated with olaparib, AZD1775, or both. Cells were cultured at 37° C in a 5% CO2 incubator for 10 days. The colonies were rinsed with PBS and stained with Coomassie blue for 3 h. The stained colonies were counted using the CellCounter plugins.

2) Alkaline comet assay

Treated cells were harvested, resuspended at 5×10^5 cells/mL in ice-cold PBS, and combined with molten LMAgarose at a ratio of 1:10. Next, the samples were moved onto comet slides and incubated at 4° C in the dark for 40 min. After dipping the slides in pre-cooled lysis solution at 4° C for 40 min, the slides were gently moved in freshly prepared alkaline unwinding solution (200 mM NaOH, 1 mM EDTA, pH >13) for 30 min at room temperature in the dark. Electrophoresis was conducted for 30 min, and the samples were dried at room temperature overnight. Next, 100 μL of diluted SYBR Green staining solution was dropped onto each circle of

agarose, and the samples were covered with a coverslip. The tail moment and intensity were measured using the Comet Assay IV program (Andor Technology, Belfast, UK). Three independent experiments were performed for each condition.

3) Annexin V/PI apoptosis assay

Cells were seeded in 60-mm dishes and treated with olaparib, AZD1775, or both. Treated cells were harvested with trypsin and resuspended in binding buffer (#556547, BD Biosciences). The apoptosis assay was performed by double staining with 1 μL Annexin V-FITC and 2 μL PI (#556547, BD Biosciences). and incubated for 15 min at RT in the dark. The cells were analyzed on a FACSCalibur flow cytometer (BD Biosciences, San Jose, CA, USA). Cells in early and late apoptosis were defined as Annexin V-FITC-positive/PI-negative and Annexin V-FITC-positive/PI-positive cells.

3. AZD1775 abrogated G2 arrest and induced early mitotic entry

1) Phospho-Histone H3 staining assay

Treated cells were harvested with trypsin and fixed with 70% ethanol for at least 4 h at 20° C. After washing with staining buffer (#420201, BioLegend, San Diego, CA, USA), 20 μL of p-HH3 antibody (#558217, BD Bioscience), and 80 μL of staining buffer were added to each sample for 20 min at room temperature. Cells were washed with staining buffer and incubated with 200 μL of staining buffer and 2 μL of RNase A for 10 min at 37° C. Next, 5 μL of propidium iodide was added, and the cells were analyzed using a FACSCalibur flow cytometer. Each experiment was repeated three times.

4. AZD1775 disrupted HR repair and enhanced the effects of olaparib

1) Immunofluorescence assay

For RAD51 and γ-H2AX foci analysis, cells were seeded on a confocal dish, incubated for 48 h, and then treated for 24 h. The cells were fixed with 4% paraformaldehyde and permeabilized with 0.3% Triton x-100. Cells were incubated with a rabbit monoclonal RAD51(#sc-398587) antibody and mouse monoclonal γ-H2AX (#05-636) antibodies overnight at 4° C. Samples were stained with fluorochrome-conjugated secondary antibody, Alexa Fluor 488 anti-rabbit (#2147635) and Alexa Fluor 594 anti-mouse (#2179228) (Invitrogen, Carlsbad, CA, USA), and counterstained with DAPI (Sigma-Aldrich, St. Louis, MO, USA). Immunofluorescence was visualized using a Zeiss LSM 800 laser scanning microscope at 40x magnification.

5. Combination treatment of olaparib with AZD1775 showed Anti-tumor growth effects in a xenograft mouse model

1) Mouse xenograft model

Animal tests were performed at the Institute for Experimental Animals, College of Medicine, Seoul National University (Seoul, Korea) according to institutional guidelines, with prior approval from the Institutional Animal Care and Use Committee. Four-week-old female athymic nude mice were purchased from Orient Bio Inc. (Gyeonggi-do, Korea). SNU869 cells (1×10^7 cells) were subcutaneously injected into each mouse. When the tumor volume reached 250 mm3, the mice were randomly divided into four groups of five mice each. Olaparib (50 mg/kg) and AZD1775 (25 mg/kg) were administered orally once a day for 4 weeks (5 days on/2 days off), and the control group was treated with vehicle (0.5% methyl cellulose, Sigma-Aldrich) via oral gavage. Body weight and tumor size were measured every other day. The tumor volume was calculated using the following formula: tumor volume = $[(\text{width})^2 \times \text{height}]/2$.

2) Immunohistochemistry (IHC)

The isolated xenograft tumor tissues were fixed in 4% paraformaldehyde and embedded in paraffin. The paraffin blocks were sectioned on glass slides, and the slides were deparaffinized and dehydrated. The samples were detected by immunohistochemical staining with p-CDK1-Y15 (AP0016) antibody, and proliferation was evaluated using an anti-Ki67 antibody (GeneTex Inc., CA, USA). Terminal deoxynucleotidyl transferase-mediated dUTP nick end labeling (TUNEL) assay-based ApopTag Plus Peroxidase *In Situ* Apoptosis Detection Kit (EMD Millipore) was used to evaluate apoptosis.

6. Statistical analysis

Statistical analyses were conducted using SigmaPlot version 10.0 (Systat Software Inc., San Jose, CA, USA). Experimental data are presented as the mean ± standard error. All statistical tests were two-sided. Differences were considered statistically significant at $p < 0.05$. The half-maximal inhibitory concentration (IC50) of the agents was also determined using the SigmaPlot software. The effects of combined drug were analyzed by calculating the combination index (CI) using CalcuSyn software (Biosoft, Cambridge, UK). CIs of <1, 1, and >1 to indicate synergistic, additive, and antagonistic effects, respectively.

Results

1. Olaparib induced DNA damage and simultaneously activated G2/M checkpoint

To assess the anti-proliferative effects of olaparib in BTC cell lines, the MTT assay was performed after treatment with olaparib for 120 h. The anti-proliferative effect of olaparib in 10 BTC cells was modest. The IC50 in four cell lines (SNU869, HuCCT-1, SNU2773 and SNU478) was between 2.96~6.49 μM, while that of the other 6 was higher than 10 μM (Fig. 1A).

Two cell lines were selected for further experiments based on the IC50 of olaparib in the MTT assay. SNU869 showed the lowest IC50, and SNU308 showed an IC50 higher than 10 μM. We observed that olaparib induced DNA damage and apoptosis by western blotting. The expression of γ-H2AX, cleavage of PARP, cleavage of caspase-7, and cleavage of caspase-3 were induced in both cell lines. (Fig. 1B).

We performed cell cycle analysis and observed an increase in G2/M phases in two BTC cell lines in a dose-dependent manner (Fig. 1C). Olaparib increased the expression or phosphorylation of

multiple proteins involved in G2/M checkpoints, including WEE1, p-CDK1, and Cyclin B1. The protein expression of p-ATR, p-ATM, p-CHK1, p-CHK2, and p21 were also increased in the two cell lines, and p-p53 was increased in SNU308 cells. These data suggest that olaparib activates p-CDK1 and causes G2 arrest in two cell lines through both p53-dependent and p53-independent pathways (Fig. 1D). Furthermore, the expression of CtIP, RAD51, and NBS1 was increased in cells treated with olaparib, implying that DNA DSB was repaired by the HR pathway (Fig. 1E).

Figure 1.

A

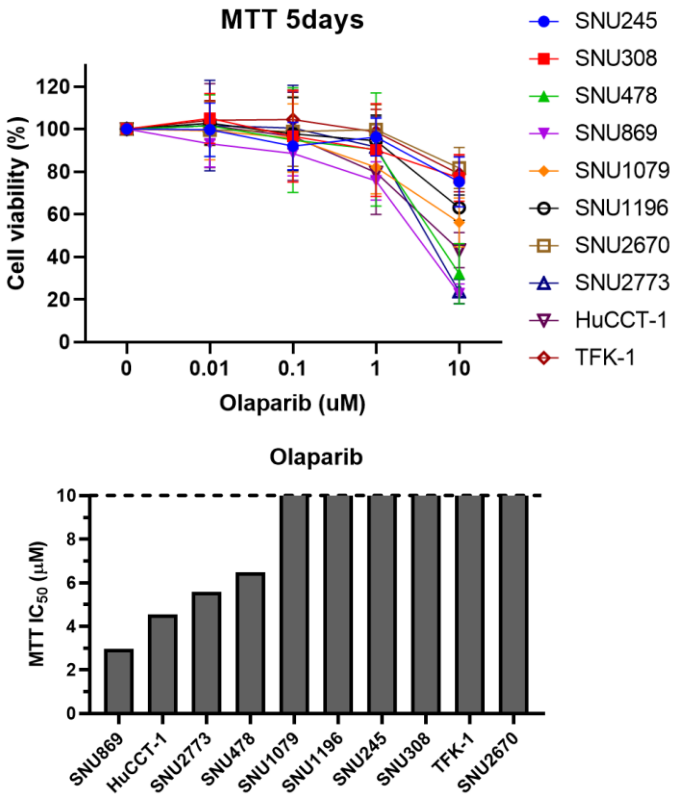
MTT 5days
Cell viability (%)
120
100
80
60
40
20
0
0
0.01
0.1
1
10
Olaparib (uM)
SNU245
SNU308
SNU478
SNU869
SNU1079
SNU1196
SNU2670
SNU2773
HuCCT-1
TFK-1
Olaparib
MTT IC50 (μM)
10
8
6
4
2
0
SNU869
HuCCT-1
SNU2773
SNU478
SNU1079
SNU1196
SNU245
SNU308
TFK-1
SNU2670

B

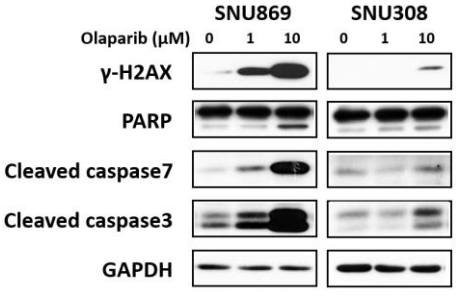
SNU869
SNU308
Olaparib (μM)
0
1
10
0
1
10
γ-H2AX
PARP
Cleaved caspase7
Cleaved caspase3
GAPDH

C

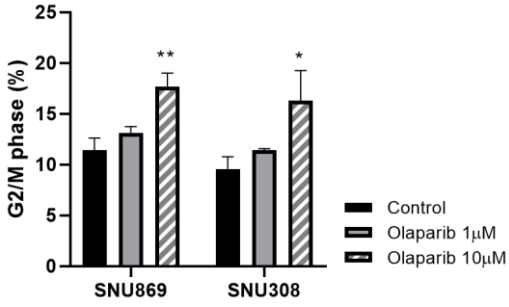
G2/M phase (%)
25
20
15
10
5
0
**
*
SNU869
SNU308
Control
Olaparib 1μM
Olaparib 10μM

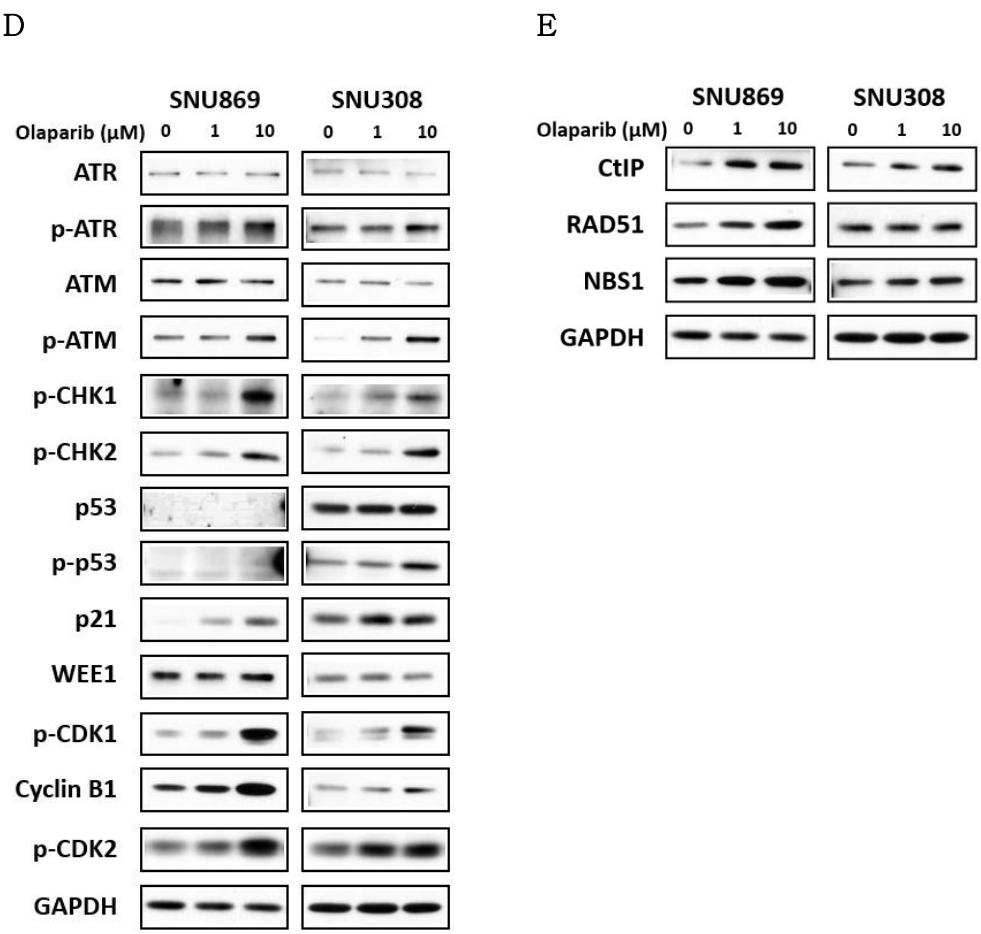

Figure 1. Olaparib induced DNA damage and simultaneously activated G2/M checkpoint

(A) MTT assay was performed in 10 BTC cell lines for 5 days after treatment with olaparib (0, 0.01, 0.1, 1, and 10 μM). The half-maximal inhibitory concentration (IC50) of olaparib was calculated using SigmaPlot. Error bars represent mean ±SD.

(B) The proteins that indicated the DNA damage and apoptosis were analyzed by western blotting after treatment with olaparib (0, 1, and 10 μM) for 72 h.

(C) Cell cycle stages were determined by flow cytometry after 72 h treatment with olaparib (0, 1, and 10 μM). Error bars represent mean ± SD. *P<0.05, **P<0.01.

(D, E) The levels of cell cycle proteins (D) and HR proteins (E) were assessed by western blotting of cells treated with 0, 1, and 10 μM olaparib for 24 h.

2. Combination therapy with olaparib and AZD1775 induced more potent DNA damage and apoptosis

We observed that olaparib induced G2 arrest, allowing cancer cells the time to repair DNA damage (Fig. 1C, Fig. 1D). For this reason, we combined olaparib with AZD1775 to inhibit CDK1. To determine the dose of combination therapy, we examined the antiproliferation of olaparib and AZD1775 as single agents in 10 BTC cell lines (Fig. 1A and supplementary Fig. 1). The average doses of IC_{50} values, except for data exceeding the maximal values, were used for *in vitro* combination therapy (Supplementary table 1). To assess the anti-proliferative effects of olaparib and AZD1775, we performed the MTT assay, in which the CI values were lower than 0.5, and synergy was found in two cell lines (Fig. 2A). The colony-forming assay also showed an increase in the anti-proliferation effect in the combination treatment (Fig. 2B). We performed the comet assay to analyze the increase in DNA damage after treatment with olaparib, AZD1775, and their combination for 72 h. The tail intensity and tail moment increased significantly after combination treatment in the SNU869 and SNU308 cell lines (Fig. 2C).

In the annexin V and cell cycle analyses, the annexin V-positive cells and the sub-G1 proportions were higher in the combination therapy than in either monotherapy (Fig. 2D, Fig. 2E). These observations indicate that the apoptosis rate was higher in the combination therapy group than in the olaparib or AZD1775 monotherapy group. In agreement with this result, the expression of γ-H2AX, cleavage of PARP, cleavage of caspase-7, and cleavage of caspase-3 were all increased in the combination therapy group than in the monotherapy groups (Fig. 2F). These data showed that adding AZD1775 to olaparib resulted in increased DNA damage and apoptosis in BTC cells.

Figure 2.

A

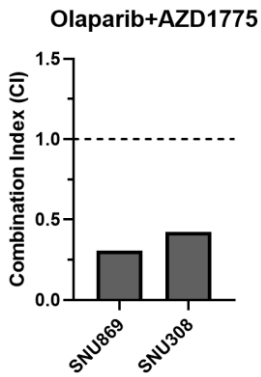
Olaparib+AZD1775
Combination Index (CI)
1.5
1.0
0.5
0.0
SNU869
SNU308

B

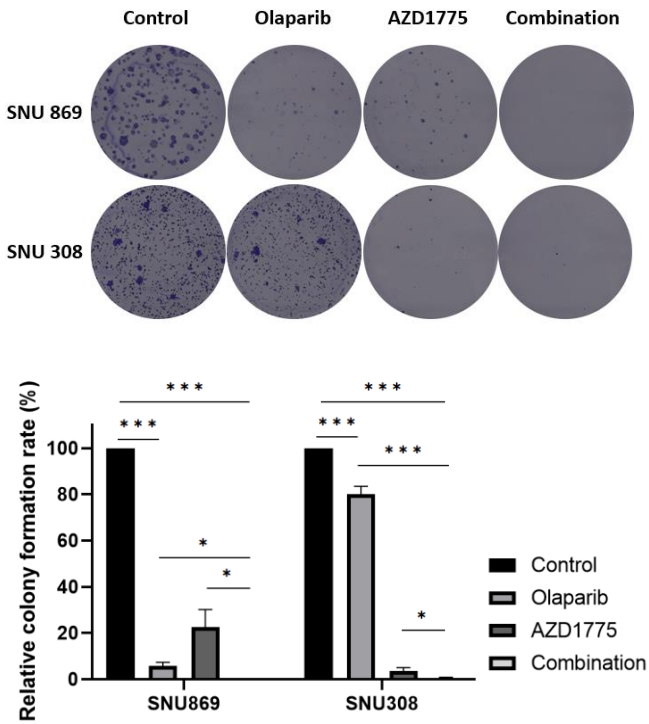
Control
Olaparib
AZD1775
Combination
SNU 869
SNU 308
Relative colony formation rate (%)
100
80
60
40
20
0
***
*
SNU869
SNU308
Control
Olaparib
AZD1775
Combination

C

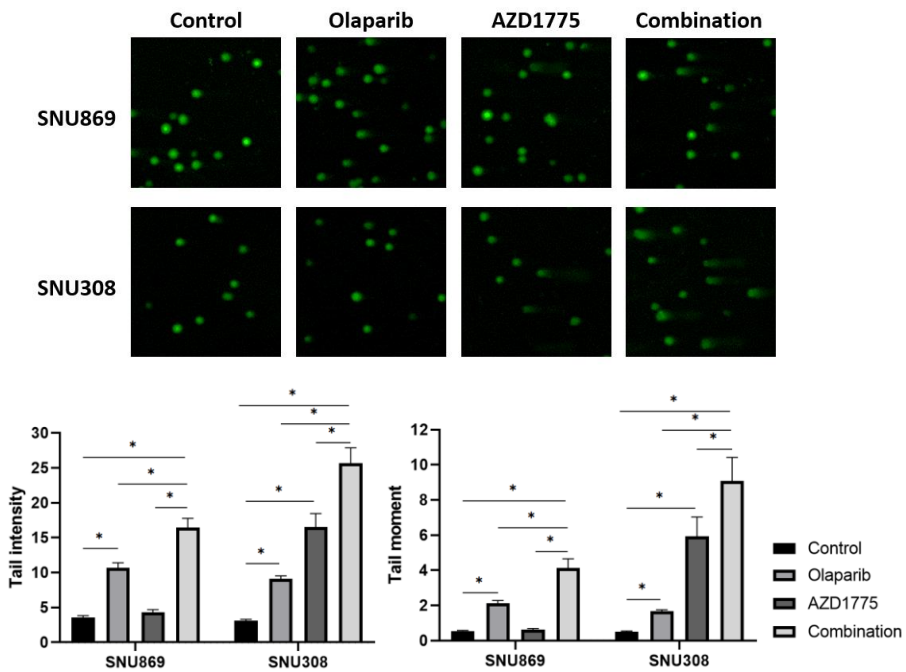
Control
Olaparib
AZD1775
Combination
SNU869
SNU308
Tail intensity
30
25
20
15
10
5
0
Tail moment
12
10
8
6
4
2
0
*
SNU869
SNU308
Control
Olaparib
AZD1775
Combination

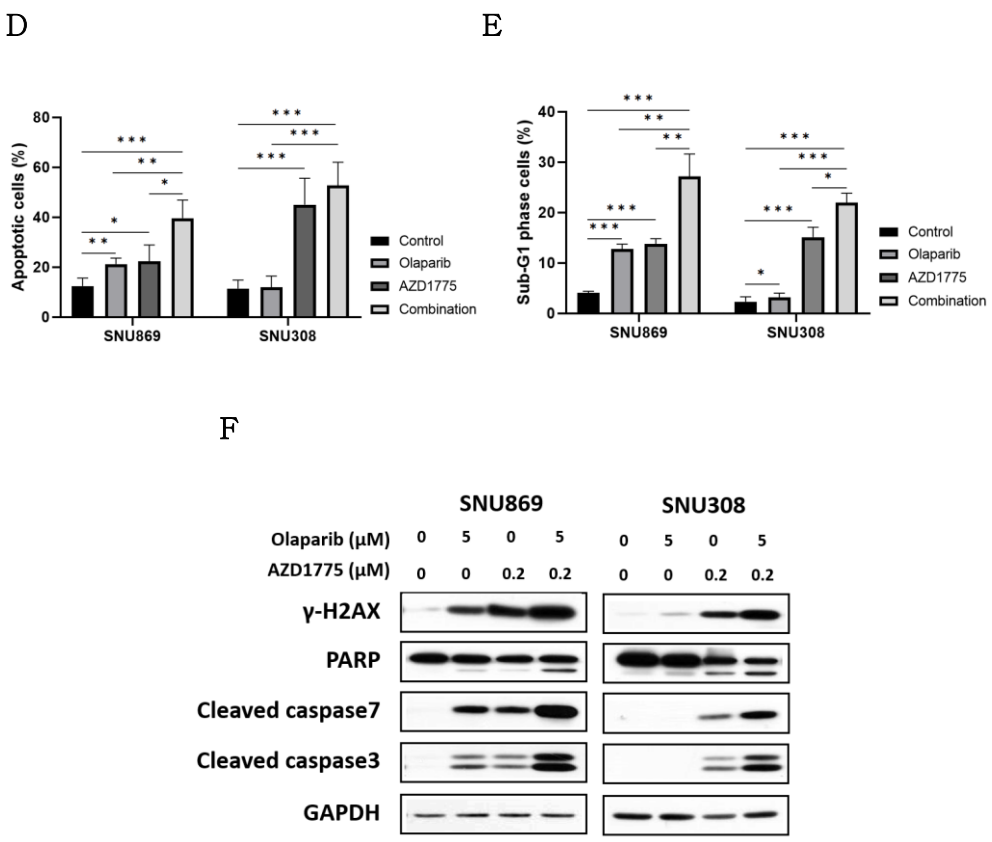

Figure 2. Combination therapy with olaparib and AZD1775 induced more potent DNA damage and apoptosis

(A) Combination effect was investigated by MTT for 5 days before treatment with olaparib (0, 0.01, 0.1, 1, and 10 μM) and AZD1775 (0, 0.001, 0.01, 0.1, and 1 μM), dose ratio was 10:1. CI value was analyzed by CalcuSyn software. If the value is lower than 1 is synergistic, and the cell lines that higher than 1 exhibit an antagonistic effect.

(B) Colony forming analysis was performed with Olaparib (5 μM), AZD1775 (0.2 μM) or both for 10 days. Error bars represent mean ±SD (n=3).

(C) Comet analysis was conducted after treatment with olaparib (5 μM), AZD1775 (0.2 μM) or both for 72 h. The tail intensity and tail moment were analyzed using the Comet assay 4(IV) program. The experiment was repeated three times. Data are expressed as mean ± SEM (n=100).

(D) Apoptosis analysis was performed using annexin V/PI double staining after 72 h treatment with olaparib (5 μM), AZD1775 (0.2 μM) or both. Error bars represent mean ±SD (n=5).

(E) Cell cycle analysis were performed with PI-stained BTC cells using flow cytometry after 72 h treatment with olaparib (5 μM), AZD1775 (0.2 μM) or both. Error bars represent mean ±SD (n=3).

(F) Western blotting of two cell lines was performed after 72 h incubation with olaparib, AZD1775, or both. *P<0.05, **P<0.01, ***P<0.001.

3. AZD1775 abrogated G2 arrest and induced early mitotic entry

As olaparib-treated cells induced G2 arrest, we hypothesized that AZD1775 might increase the sensitivity of olaparib by inducing early mitotic entry of cancer cells. We therefore performed a phospho-histone H3 staining assay to detect the increase in mitotic cells. The proportion of p-HH3-positive cells increased by AZD1775 alone or in combination, indicating an increased percentage of cells in the mitotic phase (Fig. 3A). Combination treatment with olaparib and AZD1775 increased p-ATR, p-CHK1, p-p53 and p21, but WEE1, p-CDK1, p-CDK2, and p-CDC25C expression decreased due to AZD1775. (Fig. 3B). These data showed that the inhibition of WEE1 overrode olaparib-induced G2 arrest and forced olaparib-treated cells to enter mitosis.

Figure 3.

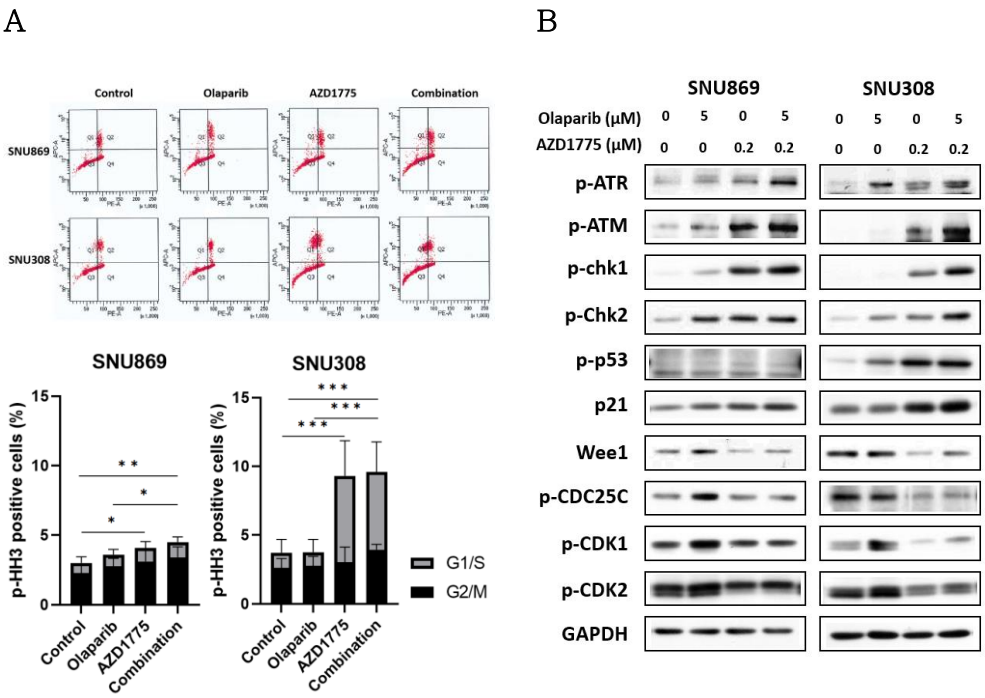

Figure 3. AZD1775 abrogated G2 phase arrest and induced early mitotic entry

(A) The phospho-histone H3 (p-HH3)-positive population was analyzed by flow cytometry after 24 h treatment with olaparib (5 μM), AZD1775 (0.2 μM), or both. The experiment was repeated five times. Error bars represent mean ±SD. *P<0.05, **P<0.01, ***P<0.001.

(B) Western blotting of cell cycle arrest-related signaling proteins was performed in BTC cells treated with olaparib (5 μM), AZD1775 (0.2 μM), or both for 24 h.

4. AZD1775 disrupted HR repair and enhanced the effects of olaparib

An immunofluorescence assay was performed to investigate the HR-disrupting effects of AZD1775. The number of γ-H2AX foci formation was more significantly increased by combination treatment with olaparib and AZD1775 than by monotherapy with either drug. On the other hand, olaparib-induced RAD51 foci formation was decreased by the combination treatment with AZD1775 (Fig. 4A). Consistent with this finding, western blotting data revealed decreased expression of RAD51 in the AZD1775 group. We also showed that AZD1775 downregulated CtIP and NBS1 level, keeping this condition in combination treatment (Fig. 4B). Our findings suggest that combination treatment with AZD1775 induced more DNA damage than olaparib monotherapy, while AZD1775 diminished DNA damage repair by blocking the HR repair process.

Figure 4.

A

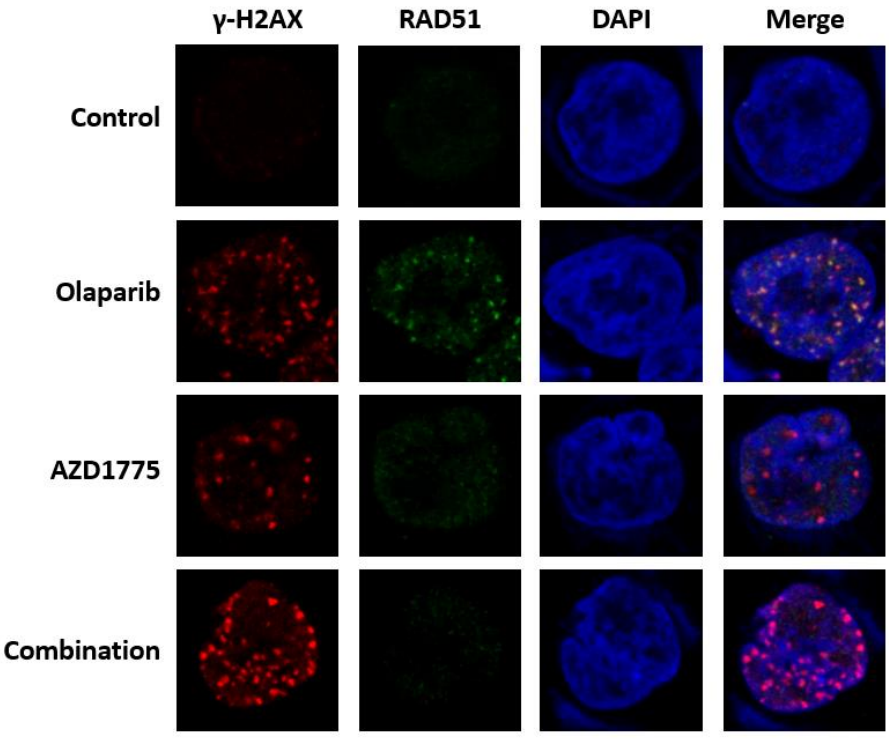
γ-H2AX
RAD51
DAPI
Merge
Control
Olaparib
AZD1775
Combination

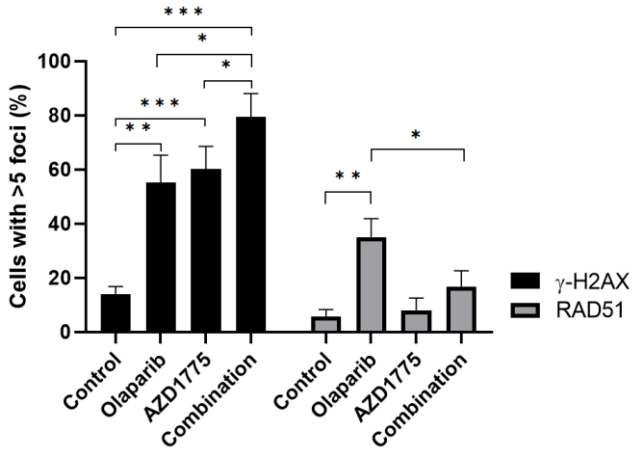
Cells with >5 foci (%)
100
80
60
40
20
0
***
*
*
***
**
**
*
Control
Olaparib
AZD1775
Combination
Control
Olaparib
AZD1775
Combination
γ-H2AX
RAD51

B

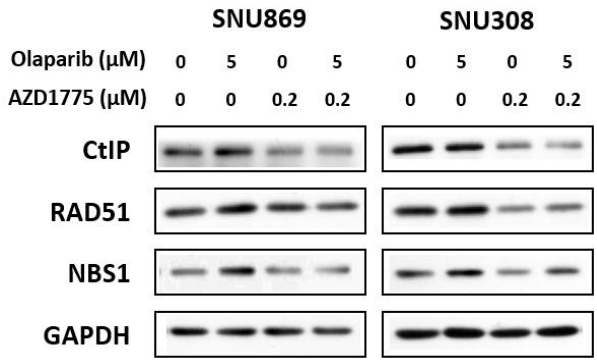

Figure 4. AZD1775 disrupted homologous recombination (HR) repair and enhanced the effects of olaparib

(A) Immunofluorescence staining of γ-H2AX (red) and RAD51 (green) in SNU869 cells treated with olaparib (5 μM), AZD1775 (0.2 μM), or a combination of olaparib and AZD1775 for 24 h. Cells with more than 5 foci were counted; 100 cells were analyzed, with experiments repeated 3 times. A confocal microscope at x400 magnification was used. Error bars represent mean ±SD. Western blotting of cell cycle arrest-related signaling proteins was performed in BTC cells treated with olaparib (5 μM), AZD1775 (0.2 μM), or both for 24 h.

(B) Western blotting was performed after 24 h treatment to show decrease in HR-related proteins.

5. Combination treatment of olaparib with AZD1775 showed Anti-tumor growth effects in a xenograft mouse model

To determine whether olaparib plus AZD1775 could exert an anti-tumor effect *in vivo*, we established a SNU869 xenograft model. Combination therapy significantly reduced tumor growth compared with that in the olaparib monotherapy and control groups. (Fig. 5A). The combination treatment was also well-tolerated (Fig. 5B). Similar to the *in vitro* results, p-ATR and p-CHK1 levels were increased by combination therapy, whereas WEE1, p-CDK1, p-CDK2, CtIP, and RAD51 were decreased by the addition of AZD1775, compared with those in the olaparib monotherapy group (Fig. 5C). Immunohistochemical staining revealed that the proliferation marker ki-67 was decreased in tumor tissues by the combination of olaparib and AZD1775. Furthermore, apoptosis was increased in combination therapy, which is represented by an increase in TUNEL staining. When we quantified the level of p-CDK1, it was decreased in combination therapy, which is consistent with our *in vitro* data (Fig. 5D). These *in vivo* results supported our *in vitro* data that dual blocking of PARP and WEE1 improved anti-tumor effects compared with those of monotherapy.

Figure 5.

A

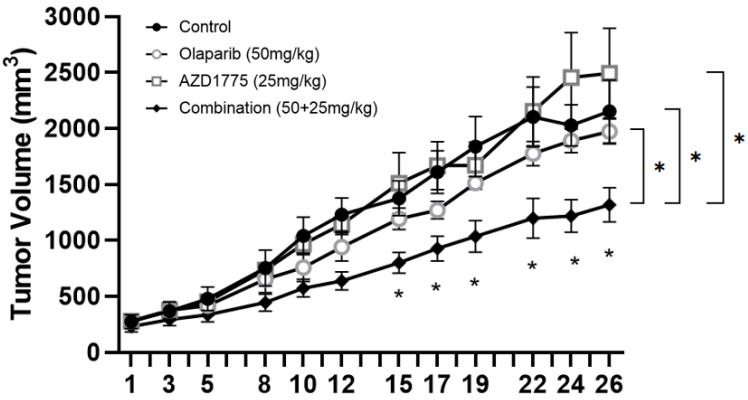
Tumor Volume (mm3)
3000
2500
2000
1500
1000
500
0
1 3 5 8 10 12 15 17 19 22 24 26
Control
Olaparib (50mg/kg)
AZD1775 (25mg/kg)
Combination (50+25mg/kg)
*

B

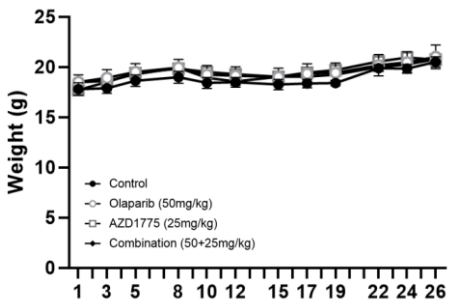
Weight (g)
25
20
15
10
5
0
1 3 5 8 10 12 15 17 19 22 24 26
Control
Olaparib (50mg/kg)
AZD1775 (25mg/kg)
Combination (50+25mg/kg)

C

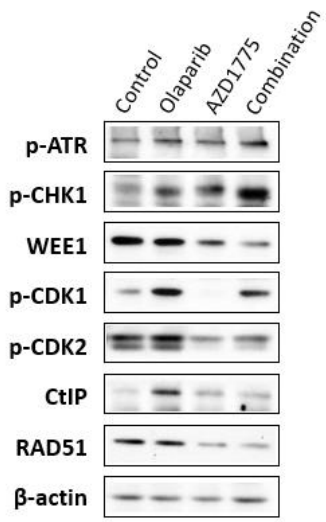
Control
Olaparib
AZD1775
Combination
p-ATR
p-CHK1
WEE1
p-CDK1
p-CDK2
CtIP
RAD51
β-actin

D

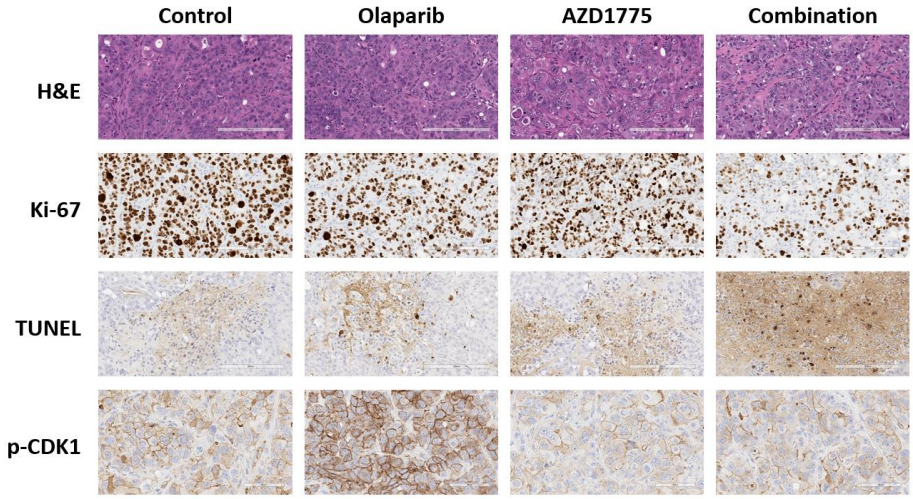

Figure 5. Combination treatment of olaparib with AZD1775 showed Anti-tumor growth effects in a xenograft mouse model

(A) Vehicle, olaparib (50 mg/kg), AZD1775 (25 mg/kg), or both drugs were administered orally once a day for 4 weeks (5 days on/2 days off) to all groups of SNU869 xenograft mice (n = 5 per group). Tumor volumes were measured three times weekly. Data are expressed as mean ± SEM.

(B) Mouse weights (n = 5 per group) were measured three times weekly. Data are expressed as mean ± SEM.

(C) Western blotting was performed for tumor-specific proteins in each group after tumor isolation.

(D) SNU869-xenografted tumors were stained with H&E (x200), Ki67 (x200), TUNEL (x200), and p-CDK1 (x400) for immunohistochemical analysis. Scale bars = 200 μm (H&E, Ki67, and TUNEL) and scale bars = 60 μm (p-CDK1).

Discussion

In this study, we have found that olaparib combined with AZD1775 can induce synergistic anti-tumor effects against BTC. Previous studies have shown that olaparib induces G2 arrest through the p53-p21-CDK1 axis [14, 22]. However, cancer cells with absent or mutated p53 could activate p53-independent pathways to regulate G2/M checkpoint. It is known that SNU869 has a p.Asp48Gly p53 mutation, and SNU308 has a p.Val217Gly p53 mutation, but the function of these mutations has not been revealed. In our previous report, the basal level of p53 was relatively low in SNU869 cells and high in SNU308 compared with that in other BTC cell lines [23]. The previous report showed that AZD1775 increased sensitivity to olaparib in tumor cells with absent or mutated p53 [24]. In our study, the effect of AZD1775 was independent of p53 expression (data not shown). Although the p53 and p-p53 levels were different between the two BTC cell lines (SNU869, SNU308), we observed that the phosphorylation of CDK1 was increased and G2 arrest was induced in olaparib-treated cells.

Based on findings of G2 arrest with olaparib monotherapy, we combined olaparib with a WEE1 inhibitor to disrupt DNA repair at the G2 phase by inhibiting CDK1 phosphorylation. Because the

CDK1/cyclin B1 complex is known as a key molecule regulating G2/M transition, AZD1775-treated cancer cells abrogate the G2/M checkpoint, leading to early mitosis entry. Furthermore, early mitosis can cause mitotic catastrophe and subsequently lead to apoptosis [16, 18]. Here we showed that AZD1775 abrogated G2 arrest by decreasing p-CDK1 expression and increasing p-HH3 positive cells. This raised the possibility that AZD1775 induced mitotic catastrophe and led to apoptosis, but we need further investigation in mitotic catastrophe experiments.

Olaparib induces DNA DSB; however, damaged DNA is mostly repaired by the HR pathway [12]. Repair of double-stranded DNA (dsDNA) damage through the HR is also known as one of the resistance mechanisms of olaparib [12]. In addition, previous studies have reported that the expression of RAD51 and CtIP regulates the sensitivity of breast cancer cells to olaparib [26, 27]. Consistent with other reports, we observed that DSB repairs through the HR pathway in olaparib-treated cancer cells, which was indicated by an increase in HR repair protein expression and accumulation of RAD51. A recent study showed that CDK1 regulates the phosphorylation of RAD51 during HR repair [28]. We

also observed that AZD1775 disrupted the HR pathway by decreasing the recruitment of RAD51 on DNA damage sites.

Additionally, CtIP initiates HR repair by interacting with the MRE11–RAD50–NBS1 complex and by promoting DNA end resection [29, 30]. Indeed, previous studies showed that CDK2 regulates CtIP, and plays an important role in the interaction with the MRE11–RAD50–NBS1 complex to initiate HR [29, 30]. Likewise, although we did not observe that the CDK2 regulates CtIP, our study showed that AZD1775 regulates CDK2 and CtIP. Taken together, the AZD1775 regulates HR repair as well as cell cycle checkpoint, so it might be a good rationale for the enhanced combination effect with olaparib.

We performed concurrent therapy with olaparib and AZD1775 at a single dose and observed the antitumor effect in *in vivo* test. For clinical development, the tolerability and safety are important issues in combination therapy. Additionally, a recent study reported that sequential treatment with olaparib and AZD1775 minimized toxicity than concurrent treatment [31]. In this study, we demonstrated the synergistic mechanism to disrupt the G2/M cell cycle checkpoint and HR repair. Further studies are also needed to determine which

dose or sequential method of combining the two drugs can lower toxicity while maintaining efficacy.

Even though BTCs harbor DDR alterations in significant amount of cases, DDR-targeted strategies for new drug development have not been much explored so far in BTC. We've pre-clinically tested the ATR inhibitor monotherapy, ATR inhibitor in combination with cisplatin, ATR inhibitor in combination with WEE1 inhibitor, PARP inhibitor in combination with ATR inhibitor and so on in BTC [24, 32]. For clinical development of DDR-targeted strategies in BTC, we are now conducting clinical trials using DDR-acting agents in advanced BTC patients (NCT04298008, NCT04298021). Further studies are needed for proving the concept of DDR-targeting strategies in BTC.

This study is the first to give preclinical evidence that dual-inhibition of PARP and WEE1 has a synergistic anti-tumor effect in BTC. This combination strategy of PARP inhibitor with WEE1 inhibitor could have the potential to be further developed clinically in patients with advanced BTC.

References

1. Gottifredi V. Targeting DNA damage response kinases in cancer therapy. Mutat Res. 2020;821:111725.
2. Tariq NU, McNamara MG, Valle JW. Biliary tract cancers: current knowledge, clinical candidates and future challenges. Cancer Manag Res. 2019;11:2623-42.
3. Ricci AD, Rizzo A, Bonucci C, Tober N, Palloni A, Mollica V, et al. PARP Inhibitors in Biliary Tract Cancer: A New Kid on the Block? Medicines (Basel). 2020;7(9).
4. Ahn DH, Bekaii-Saab T. Biliary tract cancer and genomic alterations in homologous recombinant deficiency: exploiting synthetic lethality with PARP inhibitors. Chin Clin Oncol. 2020;9(1):6.
5. Robson M, Im SA, Senkus E, Xu B, Domchek SM, Masuda N, et al. Olaparib for Metastatic Breast Cancer in Patients with a Germline BRCA Mutation. N Engl J Med. 2017;377(6):523-33.
6. Golan T, Hammel P, Reni M, Van Cutsem E, Macarulla T, Hall MJ, et al. Maintenance Olaparib for Germline BRCA-Mutated Metastatic Pancreatic Cancer. N Engl J Med. 2019;381(4):317-27.

7. Moore K, Colombo N, Scambia G, Kim BG, Oaknin A, Friedlander M, et al. Maintenance Olaparib in Patients with Newly Diagnosed Advanced Ovarian Cancer. N Engl J Med. 2018;379(26):2495-505.
8. de Bono J, Mateo J, Fizazi K, Saad F, Shore N, Sandhu S, et al. Olaparib for Metastatic Castration-Resistant Prostate Cancer. N Engl J Med. 2020;382(22):2091-102.
9. Pommier Y, O'Connor MJ, de Bono J. Laying a trap to kill cancer cells: PARP inhibitors and their mechanisms of action. Science Translational Medicine. 2016;8(362):362ps17-ps17.
10. Shrivastav M, De Haro LP, Nickoloff JA. Regulation of DNA double-strand break repair pathway choice. Cell Res. 2008;18(1):134-47.
11. Sunada S, Nakanishi A, Miki Y. Crosstalk of DNA double-strand break repair pathways in poly (ADP-ribose) polymerase inhibitor treatment of breast cancer susceptibility gene 1/2-mutated cancer. Cancer Sci. 2018;109(4):893-9.
12. Lee EK, Matulonis UA. PARP Inhibitor Resistance Mechanisms and Implications for Post-Progression Combination Therapies. Cancers (Basel). 2020;12(8).

13. Jelinic P, Levine DA. New insights into PARP inhibitors' effect on cell cycle and homology-directed DNA damage repair. Mol Cancer Ther. 2014;13(6):1645-54.

14. Taylor WR, Stark GR. Regulation of the G2/M transition by p53. Oncogene. 2001;20(15):1803-15.

15. Patil M, Pabla N, Dong Z. Checkpoint kinase 1 in DNA damage response and cell cycle regulation. Cell Mol Life Sci. 2013;70(21):4009-21.

16. Ghelli Luserna di Rora A, Cerchione C, Martinelli G, Simonetti G. A WEE1 family business: regulation of mitosis, cancer progression, and therapeutic target. J Hematol Oncol. 2020;13(1):126.

17. Schmidt M, Rohe A, Platzer C, Najjar A, Erdmann F, Sippl W. Regulation of G2/M Transition by Inhibition of WEE1 and PKMYT1 Kinases. Molecules. 2017;22(12).

18. Yang L, Shen C, Pettit CJ, Li T, Hu AJ, Miller ED, et al. Wee1 Kinase Inhibitor AZD1775 Effectively Sensitizes Esophageal Cancer to Radiotherapy. Clinical Cancer Research. 2020;26(14):3740-50.

19. Castedo M, Perfettini JL, Roumier T, Andreau K, Medema R, Kroemer G. Cell death by mitotic catastrophe: a molecular definition. Oncogene. 2004;23(16):2825-37.

20. Krajewska M, Heijink AM, Bisselink YJ, Seinstra RI, Sillje HH, de Vries EG, et al. Forced activation of Cdk1 via wee1 inhibition impairs homologous recombination. Oncogene. 2013;32(24):3001-8.

21. Nam A-R, Kim J-W, Cha Y, Ha H, Park JE, Bang J-H, et al. Therapeutic implication of HER2 in advanced biliary tract cancer. Oncotarget. 2016;7(36):58007.

22. Bunz F, Dutriaux A, Lengauer C, Waldman T, Zhou S, Brown JP, et al. Requirement for p53 and p21 to Sustain G2 Arrest After DNA Damage. Science. 1998;282(5393):1497-501.

23. Nam AR, Jin MH, Park JE, Bang JH, Oh DY, Bang YJ. Therapeutic Targeting of the DNA Damage Response Using an ATR Inhibitor in Biliary Tract Cancer. Cancer Res Treat. 2019;51(3):1167-79.

24. Xiangbing Meng, Jianling Bi, Yujun Li, Shujie Yang, Yuping Zhang, Mary Li, et al. AZD1775 Increases Sensitivity to Olaparib and Gemcitabine in Cancer Cells with p53 Mutation. Cancers (Basel). 2018;10(5):149.

25. Geenen JJJ, Schellens JHM. Molecular Pathways: Targeting the Protein Kinase Wee1 in Cancer. Clin Cancer Res. 2017;23(16):4540-4.

26. Wang J, Ding Q, Fujimori H, Motegi A, Miki Y, Masutani M. Loss of CtIP disturbs homologous recombination repair and sensitizes breast cancer cells to PARP inhibitors. Oncotarget. 2016;7(7):7701.

27. Zhao Q, Guan J, Zhang Z, Lv J, Wang Y, Liu L, et al. Inhibition of Rad51 sensitizes breast cancer cells with wild-type PTEN to olaparib. Biomed Pharmacother. 2017;94:165-8.

28. Cruz C, Castroviejo-Bermejo M, Gutierrez-Enriquez S, Llop-Guevara A, Ibrahim YH, Gris-Oliver A, et al. RAD51 foci as a functional biomarker of homologous recombination repair and PARP inhibitor resistance in germline BRCA-mutated breast cancer. Ann Oncol. 2018;29(5):1203-10.

29. Buis J, Stoneham T, Spehalski E, Ferguson DO. Mre11 regulates CtIP-dependent double-strand break repair by interaction with CDK2. Nat Struct Mol Biol. 2012;19(2):246-52.

30. Wang H, Shi LZ, Wong CC, Han X, Hwang PY, Truong LN, et al. The interaction of CtIP and Nbs1 connects CDK and ATM to

regulate HR-mediated double-strand break repair. PLoS Genet. 2013;9(2):e1003277.

31. Yong Fang, Daniel J McGrail, Chaoyang Sun, Marilyne Labrie, Xiaohua Chen, Dong Zhang, et al. Sequential Therapy with PARP and WEE1 Inhibitors Minimizes Toxicity while Maintaining Efficacy. Cancer Cell. 2019;35(6):851-867.e7.

32. Nam AR, Jin MH, Bang JH, Oh KS, Seo HR, Oh DY, et al. Inhibition of ATR Increases the Sensitivity to WEE1 Inhibitor in Biliary Tract Cancer. Cancer Res Treat. 2020;52(3):945-56.

Supplementary

Supplementary Figure S1.

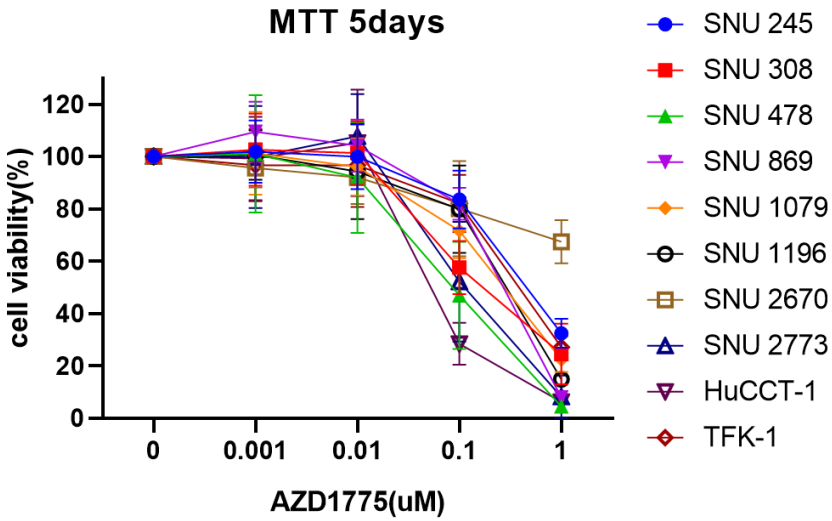

Supplementary Figure S1. The antiproliferation of AZD1775 as single agents in 10 BTC cell lines

MTT assay was performed in 10 BTC cell lines for 5 days after treatment with AZD1775 (0, 0.001, 0.01, 0.1, and 1 μM). The half-maximal inhibitory concentration (IC50) of AZD1775 was calculated using SigmaPlot. Error bars represent mean ±SD.

Supplementary Table S1.

Olaparib		AZD1775	
Cell line	IC_{50}(uM)	Cell line	IC_{50}(uM)
SNU869	2.96	HuCCT-1	0.06
HuCCT-1	4.54	SNU478	0.09
SNU2773	5.58	SNU2773	0.11
SNU478	6.49	SNU308	0.13
SNU1079	>10	SNU1079	0.21
SNU1196	>10	SNU869	0.3
SNU245	>10	SNU1196	0.32
SNU308	>10	SNU245	0.35
TFK-1	>10	TFK-1	0.41
SNU2670	>10	SNU2670	>1
Average	**4.89**	**Average**	**0.22**

Supplementary Table S1. IC_{50} of olaparib and AZD1775 in BTC cell lines

We measured the IC_{50} of olaparib and AZD1775 after performing the MTT assay. The average doses of IC_{50} values, except for data exceeding the maximal values, were used for *in vitro* combination therapy.

국문 초록

담도암에서 WEE1 억제를 통한 PARP 억제제의 항종양효과 증대

목적: 담도암 (BTC) 환자 중 최대 20%는 상동재조합 (homologous recombination)을 포함한 DNA 손상 반응 (DNA damage response) 유전자 변형이 있다고 알려져 있다. 따라서 DDR 경로를 표적으로 약을 투여하는 것이 BTC 를 치료하는 중요한 방법으로 대두되고 있다. PARP 억제제는 single-strand break (SSB) 복구를 방해하고 이 SSB 는 double-strand break (DSB)으로 전환된다. 반면, WEE1 억제제는 G2/M 세포주기 checkpoint 와 상동재조합을 통한 DNA 수리를 방해한다. 이러한 이유로 우리는 BTC 에서 PARP 및 WEE1 억제제를 동시 투여하여 항종양효과를 규명하고자 한다.

재료 및 방법: 우리는 10 개의 담도 암 세포주에서 olaparib (PARP 억제제) 및 AZD1775 (WEE1 억제제)를 처리하여 항종양효과를 *in vitro* 에서 평가하였다. Olaparib 의 효과를 보기 위해 MTT, western blotting, cell cycle assay 를 진행하였다. Olaparib 과 AZD1775 의 시너지효과를 보기 위하여 colony forming assay, alkaline comet assay, and annexin V/PI apoptosis assay 를 진행하였다. p-HH3 staining assay 를 수행하여 유사 분열 세포를 측정하고 immunofluorescence assay 를 수행하여 RAD51 foci 를 확인했다. 또한 *in vivo* 실험을 위해

SNU869 이종 이식 모델을 구축하였고 종양 조직을 이용하여 immunohistochemistry 을 수행했다.

결과: 이 연구에서 olaparib 은 BTC 에서 강하지 않은 항증식효과를 보였고 γ-H2AX 와 caspase-7 및 caspase-3 의 절단을 통해 DNA 이중 가닥 절단 (DSB)와 세포사멸이 유도됨을 확인하였다. 그러나, 우리는 세포주기 분석을 통해 G2 arrest 의 증가를 관찰하였고, G2/M checkpoint marker 인 p-CDK1 및 Cyclin B1 의 증가도 확인하였다. olaparib 에 의해 유도된 DNA DSB 는 HR 경로를 통해 복구되었고 이는 CtIP, RAD51, NBS1 발현의 증가를 통해 확인하였다. AZD1775 는 일반적으로 G2/M 확인지점을 제어하기 때문에 olaparib 과 AZD1775 를 병용투여 하였을 때 G2 확인지점을 통과하게 된다. 이는 AZD1775 가 G2/M 확인 지점의 대표적인 단백질인 p-CDK1 을 하향조절하고 초기 유사 분열 진입을 유도하는 것을 통해 규명하였다. AZD1775 는 또한 CtIP 및 RAD51 발현을 감소시키고 HR 을 통한 복구를 방해한다. In vivo 실험을 위한 이종 이식 모델에서 olaparib 과 AZD1775 병용투여 하는 것이 두 약물의 단독투여보다 종양억제에 더 효과적이었다.

결론: 이 연구는 olaparib 을 AZD1775 와 같이 투여하였을 때 BTC 에서 항종양효과가 상승하는 것을 처음으로 밝히고 있다. Olaparib 에 의해 증가한 G2 arrest 및 HR repair 이 진행되고 AZD1775 는 CDK1 인산화를 억제하여 G2 arrest 와 HR repair 진행을 방해한다. Olaparib 과 AZD1775 의 병용 요법은 in vivo 실험에서도 항 종양 효과를 보였으며 이

논문은 두 약제의 병용투여가 BTC 환자에서 임상적으로 더 개발될 가능성을 보여준다.

Keywords: PARP, WEE1, 담도암, DNA 손상 반응, 세포 주기 확인지점, 상동재조합

Student Number: 2019-28812